Electron spin resonance investigation of Mn^{2+} ions and their dynamics in Mn-doped $SrTiO_3$

V. V. Laguta,[1,3] I. V. Kondakova,[1] I. P. Bykov,[1] M. D. Glinchuk,[1] A. Tkach,[2] P. M. Vilarinho,[2] and L. Jastrabik[3]
[1]*Institute for Problems of Material Science, NASc of Ukraine, Krjijanovskogo 3, 03680 Kiev, Ukraine*
[2]*Department of Ceramics and Glass Engineering, CICECO, University of Aveiro, 3810-193 Aveiro, Portugal*
[3]*Institute of Physics, ASCR, Cukrovarnicka 10, 16253 Prague, Czech Republic*
(Received 9 February 2007; published 2 August 2007)

Using electron spin resonance (ESR), the lattice position and dynamic properties of Mn^{2+} ions were studied in 0.5 and 2 at. % manganese-doped $SrTiO_3$ ceramics prepared by the conventional mixed oxide method. The measurements show that Mn^{2+} ions preferably (up to 97%) substitute for the Sr if the ceramics are prepared with a deficit of Sr ions. Motional narrowing of the Mn^{2+} ESR spectrum was observed when the temperature increased from 120 to 240–250 K, which was explained as a manifestation of the off-center position of this ion at the Sr site. From the analysis of the ESR spectra, the activation energy $E_a=86$ mV and frequency factor $1/\tau_0 \approx (1-5)10^{13}$ s^{-1} for the jumping of the impurity between symmetrical off-center positions were determined. Both are in agreement with those previously derived from the dielectric relaxation. This proves that the origin of the dielectric anomaly in $SrTiO_3$:Mn is produced by the reorientation dynamics of Mn^{2+} dipoles.

DOI: 10.1103/PhysRevB.76.054104 PACS number(s): 77.84.Dy, 61.72.−y, 76.30.Fc

I. INTRODUCTION

Incipient ferroelectric $SrTiO_3$ (STO) is considered to be a classical displacive soft-mode system where, however, the ferroelectric phase is suppressed by zero-point quantum fluctuations of the soft mode, leading to quantum paraelectricity down to the lowest temperatures, $T \rightarrow 0$.[1] Owing to the unusually high polarizability, various types of polar phases (dipole glass, ferroglass, and ferroelectric) can be induced by dipole impurities[2] or by pressure[3] and by ^{18}O isotope exchange.[4,5] From this point of view, $SrTiO_3$ is a promising material for many applications of ferroelectrics, especially at cryogenic temperatures.

Among different types of doping impurities, those possessing both electric and magnetic dipole moments attract special attention from scientists because they allow the construction of multiferroic materials which show unusual magnetoelectric properties (for example, see Ref. 6). Recent dielectric investigations of STO ceramic samples doped with Mn^{2+} paramagnetic ions under special conditions[7] (lacking Sr^{2+} ions) have shown a strongly marked dielectric anomaly around 50 K: a diffuse maximum in the dielectric susceptibility and losses shifting to higher temperatures with increasing measurement frequency and amount of manganese, which could indicate the onset of a polar phase.[8,9] The anomaly is attributed to reorientational motion of dipoles formed in the host matrix due to a possible off-central position of Mn^{2+} impurity ions substituting for the Sr^{2+} ions.[8,9] However, more direct evidence is necessary to prove this idea, and more detailed information about the dipoles created by a Mn impurity in the lattice should be obtained. Electron spin resonance (ESR) is the most direct method for determination of paramagnetic impurity center structure and characteristics. So, taking into account that Mn^{2+} is a paramagnetic ion, it would be very fruitful to carry out ESR measurements.

ESR studies of Mn impurities in STO have been performed previously by several authors. Because of the multivalent character of Mn ions, several types of manganese center were found and described in both single crystals[10,11] and ceramics.[12] Usually the manganese dissolves into $SrTiO_3$ as Mn^{4+} ($3d^3, S=3/2$), which naturally substitute for Ti^{4+}.[10] However, in $SrTiO_3$:Mn ceramics[12] and in reduced $SrTiO_3$:Mn single crystals,[11] Mn^{2+} ($3d^5, S=5/2$) ESR spectra have also been observed. All these spectra were assigned to Mn^{2+} substituted for Ti^{4+} with (and without) local charge compensation. Because the ionic radius of Mn^{2+} (0.83 Å) is higher than that of Ti^{4+} (0.605 Å),[13] it is hardly to be expected that in such a substitution the manganese will be off-centrally shifted. On the other hand, recent reports on the structure and microstructure of $SrTiO_3$:Mn ceramics clearly indicate that manganese ions can be incorporated at both Sr and Ti sites of the STO lattice, depending on the starting stoichiometric composition.[7,14] Therefore, the origin of the manganese dipole centers in $SrTiO_3$ is still not clear and calls for detailed investigation.

In the present work, we report a detailed ESR study of ceramic samples with nominal composition $Sr_{1-x}Mn_xTiO_3$ ($x=0$, 0.5, and 2 at.%). Quantitative analysis of the measured Mn^{2+} ESR spectra shows that manganese preferably substitutes for the Sr ions, and Mn^{2+} displacement from the central position in the STO cubic lattice in several symmetrical directions creates reorientational dipoles. These Mn^{2+}_{Sr} dipoles are responsible for the dielectric anomaly observed around 50 K (for Mn concentration of 2 at. % and frequency of 10 kHz) as dielectric relaxation. The parameters describing the dipole-relaxation dynamics are determined by ESR analysis, being approximately the same as those obtained by dielectric spectroscopy analysis.

II. SAMPLES AND EXPERIMENTAL DETAILS

Ceramic samples were prepared by the conventional mixed oxide method. Reagent grade $SrCO_3$, TiO_2, and MnO_2 were weighed according to the compositions $Sr_{1-x}Mn_xTiO_3$ with $x=0$, 0.005, and 0.02 (for details, see Ref. 7). Room-temperature structural analysis[7] indicated that all of the samples are of single cubic perovskite phase.

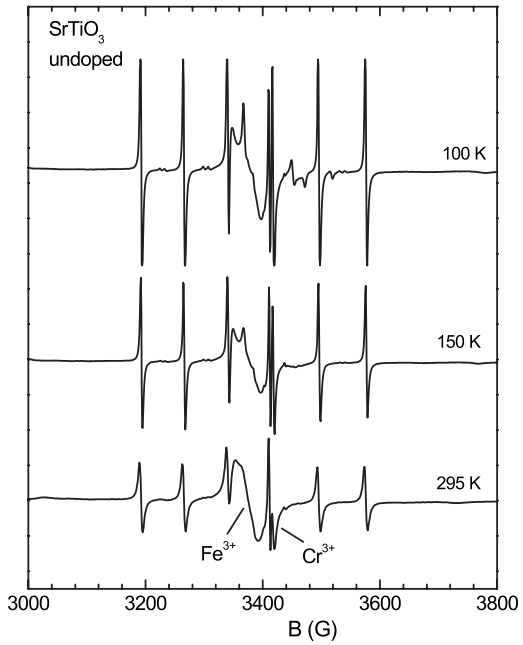

FIG. 1. ESR spectra of undoped $SrTiO_3$ ceramics taken at several temperatures. Six narrow lines arise from Mn^{4+} ions.

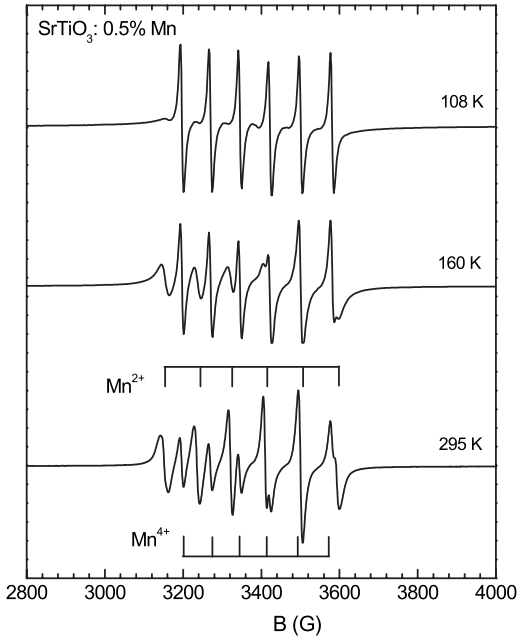

FIG. 2. ESR spectra of $SrTiO_3$:0.5% Mn ceramics taken at several temperatures.

ESR measurements were performed at 9.5–9.6 GHz in the standard 3 cm wavelength range and at a temperature of 20–300 K. An Oxford Instrument ESR 900 cryosystem was used.

III. EXPERIMENTAL RESULTS

Even undoped $SrTiO_3$ ceramic samples show the ESR spectrum of a Mn^{4+} impurity (Fig. 1) which substitutes for Ti^{4+}. The spectrum was well described by a spin Hamiltonian with isotropic g factor 1.9920 ± 0.0002 and hyperfine constant $A=(71.3\pm0.1)\times10^{-4}$ cm^{-1} (the ^{55}Mn isotope has nuclear spin $I=5/2$) similar to those published by Müller.[10]

Besides the Mn^{4+} impurity, the samples also contained some amount of Fe^{3+} and Cr^{3+} ions (shown in Fig. 1, too), which both substitute for Ti^{4+} as well. All these spectra show a conventional behavior with decrease of the temperature, which is characteristic of the Ti cubic site, i.e., increase of the intensity due to decrease of the linewidth and change of the Boltzmann factor. Note that in single crystals of $SrTiO_3$ below the temperature of the structural phase transition $T_a \approx 105$ K, ESR spectra become slightly anisotropic (for example, see Ref. 11). However, this anisotropy can hardly be observed in ceramics.

In $SrTiO_3$ ceramics specially doped with Mn^{2+} ions along with Mn^{4+} spectrum another spectrum arises that is also related to manganese ions (Figs. 2 and 3). The new spectrum increases in intensity with increasing Mn concentration. Note that the integral intensity of the Mn^{4+} spectrum also increases but not as much as the intensity of the new spectrum, which we ascribe to Mn^{2+} ions substituting for Sr^{2+}. The ratio of the integral intensities of Mn^{2+} and Mn^{4+} spectra is 4.5 and 35 for 0.5% and 2% Mn, respectively. The Mn^{2+} spectrum at $T>100$ K is also described by a spin Hamiltonian of the cubic symmetry with the following spectral parameters: $g=2.0032\pm0.0002$ and $A=(82.8\pm0.2)\times10^{-4}$ cm^{-1}. No fine structure splitting of the spectrum was observed at these temperatures.

An unexpected feature of the Mn^{2+} spectrum is that the width of each line of the Mn^{2+} sextet increases nearly exponentially on lowering the temperature (Fig. 4). This is well seen in the spectrum of the sample with 2% Mn (Fig. 3),

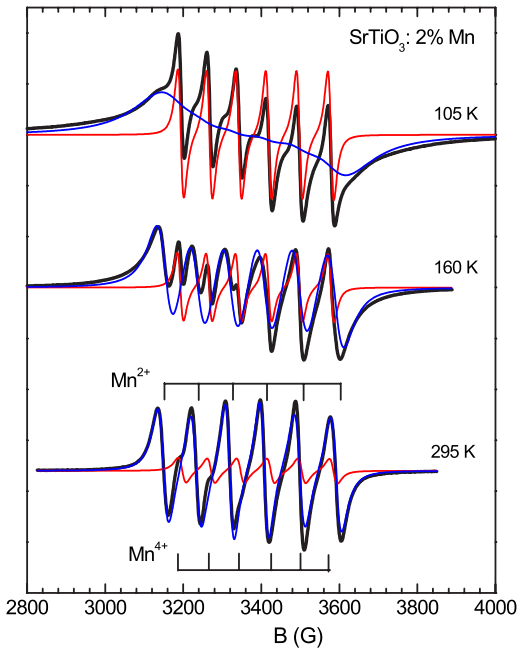

FIG. 3. (Color online) ESR spectra of $SrTiO_3$:2% Mn ceramics taken at several temperatures (thick lines). Deconvolution of the experimental spectra into two sextets belonging to Mn^{2+} and Mn^{4+} is shown by thin lines.

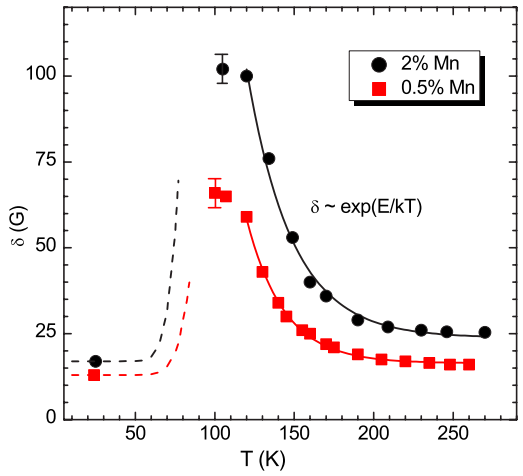

FIG. 4. (Color online) Temperature dependence of Mn^{2+} $M_s = \pm 1/2$ transition linewidth (half width at half maximum) for two manganese concentrations, 0.5% and 2%. Linewidths at 25 K were derived from "static" powder spectra by using Eq. (3).

where the broadening at $T < 130$ K is so large that the hyperfine (hf) lines become completely unresolved. At the same time one can see that the Mn^{4+} linewidth does not change with temperature. The precise values of Mn^{2+} linewidth were calculated by performing a deconvolution of the measured spectra into separated lines of Mn^{2+} and Mn^{4+} hf sextets as illustrated in Fig. 3 for the sample with 2% Mn. Note that at all temperatures the line shape is Lorentzian. The temperature dependence of the linewidth, obtained in such a way, is shown in Fig. 4 for both concentrations of manganese. The residual linewidth at high temperatures mainly originates from the dipole-dipole interaction of Mn^{2+} magnetic moments with each other and with Mn^{4+}; it is indeed larger in the sample with 2% Mn.

Such temperature behavior of the linewidth can indicate a motional narrowing of the spectrum, when impurity ions substitute for host ions in an off-center position, and thus there can be fast jumping of dipoles between several symmetrically equivalent configurations, leading to a smearing of the fine structure splitting of the spectrum, which is expected for a noncubic position of the impurity. In this sense, the observed behavior of the Mn^{2+} spectrum is very similar to the one observed in $KTaO_3$:Mn, where Mn^{2+} is off-center substituted for K^+ ion (for details, see Ref. 15).

Because the measured spectral parameters, the g factor and hyperfine constant A, are typical for the +2 charge state of manganese in perovskites (for example, see Refs. 11 and 15–20), there are no doubts that we are really dealing with Mn^{2+} ions. Moreover, very similar spectra were observed previously in Mn-doped $SrTiO_3$ single crystals[11] and ceramics.[12] However, as was pointed above, all these spectra were ascribed to Mn^{2+} at Ti^{4+} lattice sites. Therefore, the question arises whether the Mn^{2+} ions in our ceramic samples (and maybe in the other studies mentioned) really substitute for Sr^{2+} or occupy Ti^{4+} octahedral sites.

Our assignment of the Mn^{2+} spectrum as belonging to Mn^{2+} at Sr^{2+} sites is supported by the following arguments.

(i) The specimens were synthesized with a deficit of Sr ions according to the compositions $Sr_{1-x}Mn_xTiO_3$ and therefore the manganese ions preferably occupy the Sr lattice sites (for details, see Refs. 7 and 14). In particular, this was supported by x-ray and electron diffraction, and local structure analysis by transmission electron microscopy together with local chemical characterization by energy-dispersive spectroscopy, which showed that the solid solubility for Mn at the Sr site of $SrTiO_3$ is about 2% without formation of a $MnTiO_3$ phase.

(ii) The hyperfine splitting constant $A = 83 \times 10^{-4}$ cm^{-1} is too large for Mn^{2+} at the octahedral position, where the typical value is lower: for example, $|A| = (79.3-80.6) \times 10^{-4}$ cm^{-1} in $BaTiO_3$ (Refs. 17–19) and 81.0×10^{-4} cm^{-1} in MgO.[20] On the other hand, in $KTaO_3$, Mn^{2+} at the K^+ site has $A = 84 \times 10^{-4}$ cm^{-1},[15] which is quite close to the hyperfine splitting measured in this work for Mn^{2+} in $SrTiO_3$. The Sr site is dodecahedrally coordinated by O^{2-} ions; therefore the expected hyperfine splitting has to be larger than that for the Ti^{4+} octahedral site.[21]

(iii) The marked difference in ionic radii between the 12-coordinated Sr^{2+} (1.44 Å) and Mn^{2+} (1.25 Å, as obtained by extrapolation of the Shannon data[13] to larger coordination number) favors an off-center position of the Mn^{2+} ions and can explain the motional narrowing in its ESR spectrum. This is also in agreement with the slight compression of unit cell earlier observed.[7] Dielectric experiments suggest the off-centrality of Mn^{2+} ions too.[9] The difference in ionic radii between Ti^{4+} and Mn^{2+} is insufficient to induce the appearance of dynamically disordered Mn^{2+} ions shift from the central position.

IV. ANALYSIS OF THE EXPERIMENTAL DATA AND DISCUSSION

The observed spectral transformation with increasing temperature from 110 to 250 K can be explained as the manifestation of a dynamic process involving Mn^{2+} impurities. A theoretical description of the ESR spectrum behavior in the presence of impurity hopping is given in many publications (for example, see Refs. 16, 22, and 23). In our analysis we will use the results of Ref. 16 where the investigation of motional narrowing of ESR lines was performed for the case of an $S = 5/2$ paramagnetic ion hopping between three magnetically nonequivalent positions. This is adequate to our case when the paramagnetic off-center ion jumps near the central position.

We start from analysis of the ESR spectra at temperatures low enough ($T \ll 120$ K) that the dynamic process is too slow to affect the line shape (the so-called static regime). In the static regime, the Mn^{2+} spectrum has to be described by the static spin Hamiltonian which contains zero-field-splitting (ZFS) terms. It can be presented in the form

$$\hat{H} = g\beta \mathbf{B} \cdot \hat{\mathbf{S}} + A\hat{\mathbf{S}} \cdot \hat{\mathbf{I}} + D\left(\hat{S}_z^2 - \frac{1}{3}S(S+1)\right). \quad (1)$$

Here we assumed axial symmetry of the paramagnetic center (this is true at least down to the temperature of $T_a \cong 105$ K, which could, however, be shifted in Mn-doped STO). The axial crystal-field constant D reflects the local

distortion of the lattice around the Mn^{2+} ion. In the present case, it is determined by the off-center shift of the ion, which can occur in several equivalent symmetrical directions, so that the axial **Z** axis has different orientations relative to the external magnetic field. This allows one to determine the direction of the ion displacement from single-crystal spectra. However, it cannot be done in ceramics or powders because their spectrum is averaged over all crystallite orientations. Moreover, we are not able to determine the ZFS constant D by conventional means, i.e., from the positions of the fine $M_s \neq 1/2$ transitions, because no fine structure is visible in the Mn^{2+} spectrum due to the strong broadening of these transitions that usually occurs in ceramics. However, the value of D can be estimated from the shift of the central transition resonance field, which value for the conditions $|D|, |A| \ll g\beta B$ can be represented in the form[24]

$$B_r(1/2 \leftrightarrow -1/2, m) = B_0(m) + \frac{2D^2}{B_0}(8\sin^2\theta - 9\sin^4\theta) - 2m\left(\frac{D^2 A}{B_0^2}(72\sin^2\theta - 73\sin^4\theta) + \frac{2DA^2}{B_0^2}(3\cos^2\theta - 1)\right) + \cdots, \quad (2)$$

where $B_0(m)$ is the unperturbed resonance field of the mth hyperfine transition, and θ is the angle between the axial axis of the center and magnetic field. When $|D| > |A|$, we can keep in Eq. (2) only the first two largest terms. In this case, the maximum shift of the resonance field is determined by the ratio $2D^2/B_0$, which we can use for a crude approximation of the Mn^{2+} hf linewidths at $T \simeq 100-120$ K. This leads to the following values of the constant D calculated from the data of Fig. 4: 280×10^{-4} and 340×10^{-4} cm^{-1} for 0.5% and 2% manganese, respectively.

A more accurate determination of the constant D was carried out using the splitting of the hyperfine lines which appears in the static spectrum at $T \leqslant 50-60$ K. This splitting, shown in Fig. 5 by arrows, is clearly visible only for the left-hand $(1/2,5/2 \leftrightarrow -1/2,5/2)$ transition because other transitions are overlapped with strong Mn^{4+} resonances. For simulation of the static spectrum we applied the standard method by averaging the angular-dependent single-crystal spectra:

$$I(B) \propto \sum_{m=-5/2}^{m=5/2} \int_0^{\pi/2} \frac{dB_r(1/2,m)}{d(h\nu)} F\left(\frac{B_r(1/2,m) - B}{\delta}\right) \sin\theta \, d\theta, \quad (3)$$

where $B_r(1/2,m)$ is defined by Eq. (2) and $F((B_r - B)/\delta)$ is the line shape function, which was taken to be Lorentzian. Owing to the weak angular dependence of the central transition, the term $dB_r/d(h\nu)$ was treated as a constant. Contributions from the forbidden transitions were ignored too, due to their relatively small intensity when $D \ll g\beta B$.

The simulated powder spectra of the central-transition region are shown in Figs. 5(b) and 5(c), respectively for only the single Mn^{2+} and the sum of the Mn^{2+} and Mn^{4+} spectra. The best agreement between calculated and measured spectra

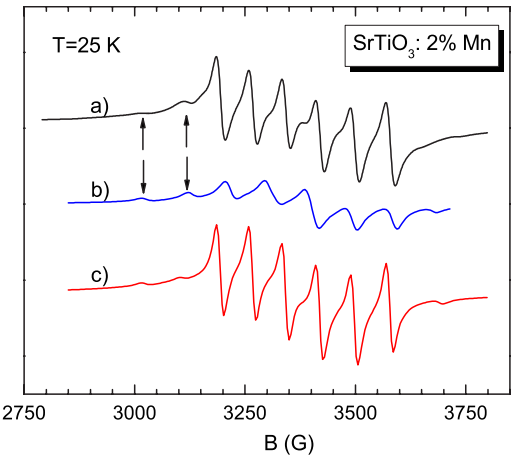

FIG. 5. (Color online) Experimental (a) and simulated (c) ESR spectra (central lines $M_S = 1/2 \leftrightarrow M_S = -1/2$) of $SrTiO_3$:2%Mn in the static regime at 25 K. The spectrum (b) represents only simulated Mn^{2+} resonances while the spectrum (c) allows also for a Mn^{4+} contribution. The splitting of the $(1/2,5/2 \leftrightarrow -1/2,5/2)$ transition is shown by arrows.

was obtained taking for Mn^{2+} $D = 420 \times 10^{-4}$ cm^{-1} and linewidth $\delta = 1.8$ mT. The obtained value of the constant D seems quite reasonable if we take into account that in $SrTiO_3$ the difference between ionic radii of Sr^{2+} and Mn^{2+} is smaller than that between K^+ and Mn^{2+} in $KTaO_3$, where the D constant is larger, 0.148 cm^{-1}.[15,16]

It should be noted that some contribution from the tetragonal distortion of the lattice to the D constant below the temperature 105 K seems to be present as well. However, our estimation of its value based on ESR data for Gd^{3+},[25] which substitutes for Sr^{2+} in the central position, shows that below the antiferrodistortive phase transition the D constant can be changed in value only by $(30-50) \times 10^{-4}$ cm^{-1}, which is much smaller with respect to the measured value 420×10^{-4} cm^{-1}. We can thus neglect this mechanism in our analysis.

As the temperature is raised and thus the rate of Mn jumps, $1/\tau$, between off-center positions increases, the fine structure components, which could be detected in the single crystal, start to broaden and finally completely disappear when the jumping rate exceeds the zero-field splitting, $1/\tau > 2D$. On further heating, all transitions merge around the central $M_S = -1/2 \leftrightarrow M_S = 1/2$ transition and give rise to a single isotropic spectrum, so that the motional averaging of the spectrum occurs. This occurs at temperatures 100–120 K (Fig. 4) and corresponds to the limit $2D < 1/\tau \leqslant \nu_0$, where $\nu_0 \simeq 9.5 \times 10^9$ Hz is the microwave frequency. However, in ceramics the central transition spectrum is predominantly inhomogeneously broadened and does not "feel" this motion of the impurity because the motional broadening cannot exceed the value D^2/B_0. Here, however, one can expect the changing of the broadening mechanism from inhomogeneous to homogeneous at $1/\tau > 2D$. As can be seen from Fig. 4, the width of hyperfine components begins to change only at $T > 120$ K, where the motional narrowing phenomenon starts at the condition $1/\tau(T) > \nu_0 \sim 10^{10}$ s^{-1}. Obviously, in this fast jump limit (so-called relaxation limit), the description of

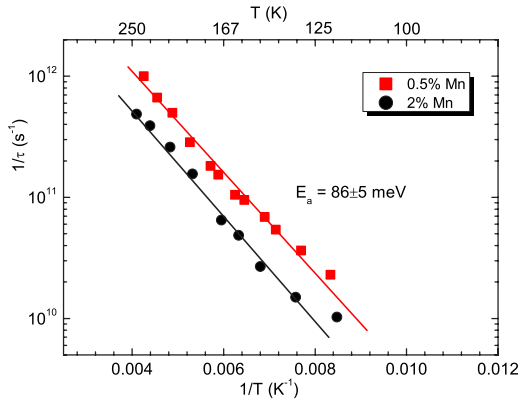

FIG. 6. (Color online) The hopping rate of Mn^{2+} dipoles in $SrTiO_3$ as a function of the reciprocal absolute temperature for two manganese concentrations 0.5% and 2%. The points were derived from the experimental spectra as described in the text. Slopes of the straight lines correspond to the activation energy E=86 meV of Mn^{2+} hopping between off-center positions in the $SrTiO_3$ lattice [see Eq. (6)].

ESR spectra in single crystals and ceramic samples becomes completely identical, because all fine transitions merge with the central transition and the spectrum becomes completely isotropic. According to Ref. 16, in the relaxation regime the shape of each motionally narrowed hyperfine line is a single Lorentzian,

$$I(B) = \frac{I_0(\delta_r + \delta_0)}{(B - B_r)^2 + (\delta_r + \delta_0)^2}, \tag{4}$$

where δ_r is the motionally narrowed linewidth and $\delta_0 \simeq 1.8$ mT is the residual linewidth. The linewidth δ_r for an $S=5/2$ ion can be written[16] as

$$\delta_r \simeq 2.8D^2\tau, \tag{5}$$

where τ is the relaxation time of ion hopping. This formula was used by us for the extraction of the relaxation time τ from the temperature dependence of narrowed ESR spectra lines. The result is shown in Fig. 6 as the dependence of the relaxation rate $1/\tau$ vs the reciprocal temperature.

One can see that the temperature dependence of the jumping rate of impurity follows well the exponential law and can be described by an Arrhenius behavior

$$\frac{1}{\tau} = \frac{1}{\tau_0}\exp(-E_a/kT) \tag{6}$$

for both 0.5% and 2% Mn-doped samples with the following kinetic parameters: the barrier height E_a=86±5 meV, and relaxation time prefactor $\tau_0 \approx 1.0 \times 10^{-13}$ and $\approx 1.8 \times 10^{-14}$ s for 0.5% and 2% Mn concentration, respectively.

The comparison of these values with the kinetic parameters obtained from the dielectric measurement data[9] shows a good coincidence, at least for the sample with 2% Mn. For lower Mn concentration the barrier height calculated from dielectric relaxation gradually decreases down to 34 mV at a doping level of 0.25%. In our opinion, this difference of ESR and dielectric measurement data is related to the fact that at low Mn concentration other relaxation mechanisms and sources can dominate in the dielectric response.[26] This is also supported by the fact that the fraction of Mn^{2+} ions is lower for the lower concentration of manganese and may be comparable to the concentration of any other impurities or defects in the sample. On the other hand, in the case of ESR, only relaxation dynamics of Mn^{2+} ions are measured. Moreover, because the homogeneous linewidth δ_r is directly proportional to the relaxation time τ, the calculated barrier height is not sensitive to the model of the ZFS constant calculation. The small difference for the relaxation time preexponent value with the change of Mn concentration obtained from the description of the temperature dependence of linewidth can be related to the interaction between dipole moments. Similar behavior was observed in the dielectric measurements.[9]

V. CONCLUSIONS

ESR investigations of ceramic samples with nominal compositions $Sr_{1-x}Mn_xTiO_3$ provided convincing evidence for the dominant occupation of the Sr site by Mn^{2+} ions. Moreover, the dielectric relaxation observed in these samples and attributed to a dynamic process involving random jumps of Mn^{2+}_{Sr} off-center ions was supported by the ESR analysis presented in this work. Particularly, (i) motional narrowing of the Mn^{2+} ESR spectrum was observed when the temperature increases from 120 to 240 K; (ii) the activation energy E_a=86 mV and frequency factor $1/\tau_0 \approx 2.5 \times 10^{13}$ s^{-1} for the jumping of the Mn^{2+} between symmetrical off-center positions deduced from ESR data are in agreement with those obtained by dielectric spectroscopy analysis.

Although our study was not able to find the direction of the Mn^{2+} off-center displacement, one can assume with high probability that it occurs at simple ⟨100⟩ cubic directions. This follows from the fact that in another very similar quantum paraelectric, $KTaO_3$, all known dipole impurities situated at the K site [for example, Li^+, Na^+, and Mn^{2+} (Ref. 2)] are always shifted along ⟨100⟩ axes. Obviously, this problem could be definitively resolved by measurements of a $SrTiO_3$:Mn^{2+} single crystal. However, to our knowledge, Mn^{2+} ESR spectra in $SrTiO_3$ single crystals have been observed only in reduced crystals,[11] which suggests that conversion of Mn^{4+} into Mn^{2+} took place, i.e., Mn^{2+} probably substituted for the Ti ions. Low-temperature ESR spectra of such Mn^{2+} ions have still not been interpreted due to the small resolution of their spectral lines. Obviously, single-crystal growth technology does not allow one to control the distribution of Mn ions between Ti and Sr sites.

ACKNOWLEDGMENTS

This work was financially supported by MSMT CR, Project No. 1M06002 and Science and Technology Center in Ukraine, Project No. 3306. The authors (A.T. and P.M.V.) acknowledge financial support from FCT, FEDER, and the European Network of Excellence FAME under Contract No. FP6-500159-1.

[1] K. A. Müller and H. Burkard, Phys. Rev. B **19**, 3593 (1979); see also W. Zhong and D. Vanderbilt, *ibid.* **53**, 5047 (1996).
[2] G. A. Samara, J. Phys.: Condens. Matter **15**, R367 (2003).
[3] H. Uwe and T. Sakudo, Phys. Rev. B **13**, 271 (1967).
[4] M. Itoh, R. Wang, Y. Inaguma, T. Yamaguchi, Y. J. Shan, and T. Nakamura, Phys. Rev. Lett. **82**, 3540 (1999).
[5] V. V. Laguta, R. Blinc, M. Itoh, J. Seliger, and B. Zalar, Phys. Rev. B **72**, 214117 (2005).
[6] M. Fiebig, J. Phys. D **38**, R123 (2005).
[7] A. Tkach, P. M. Vilarinho, and A. L. Kholkin, Acta Mater. **53**, 5061 (2005).
[8] A. Tkach, P. M. Vilarinho, and A. L. Kholkin, Appl. Phys. Lett. **86**, 172902 (2005).
[9] A. Tkach, P. M. Vilarinho, A. L. Kholkin, A. Pashkin, S. Veljko, and J. Petzelt, Phys. Rev. B **73**, 104113 (2006).
[10] K. A. Muller, Phys. Rev. Lett. **2**, 341 (1959).
[11] R. A. Serway, W. Berlinger, K. A. Müller, and R. W. Collins, Phys. Rev. B **16**, 4761 (1977).
[12] C. B. Azzoni, M. C. Mozzati, A. Paleari, V. Massarotti, M. Bini, and D. Capsoni, Solid State Commun. **114**, 617 (2000).
[13] R. D. Shannon, Acta Crystallogr., Sect. A: Cryst. Phys., Diffr., Theor. Gen. Crystallogr. **32**, 751 (1976).
[14] A. Tkach, P. M. Vilarinho, and A. L. Kholkin, Acta Mater. **54**, 5385 (2006).
[15] V. V. Laguta, M. D. Glinchuk, I. P. Bykov, J. Rosa, L. Jastrabik, M. Savinov, and Z. Trybula, Phys. Rev. B **61**, 3897 (2000).
[16] I. Laulicht, Y. Yacobi, and A. Baram, J. Chem. Phys. **91**, 79 (1989).
[17] H. Ikushima, J. Phys. Soc. Jpn. **21**, 1866 (1966).
[18] R. Bottcher, C. Klimm, D. Michel, H.-C. Semmelhack, G. Volkel, H.-J. Glasel, and E. Hartmann, Phys. Rev. B **62**, 2085 (2000).
[19] B. Milsch, Phys. Status Solidi A **133**, 455 (1992).
[20] E. R. Feher, Phys. Rev. **136**, A145 (1964).
[21] E. Simanek and K. A. Muller, J. Phys. Chem. Solids **31**, 1027 (1970).
[22] C. S. Johnson, in *Advances in Magnetic Resonance*, edited by J. S. Waugh (Academic Press, New York, 1965), Vol. 1, pp. 33–102.
[23] S. Maniv, A. Reuveni, and Z. Luz, J. Chem. Phys. **66**, 2285 (1977).
[24] J. Kliava, Phys. Status Solidi B **134**, 411 (1986).
[25] L. Rimai and G. A. deMars, Phys. Rev. **127**, 702 (1962).
[26] R. Viana, P. Lunkenheimer, J. Hemberger, R. Bohmer, and A. Loidl, Phys. Rev. B **50**, 601 (1994).